Journal of Molecular Structure 1158 (2018) 245–254

Contents lists available at ScienceDirect

Journal of Molecular Structure

journal homepage: http://www.elsevier.com/locate/molstruc

FT-IR, FT-Raman and UV–visible spectra of potassium 3-furoyltrifluoroborate salt

Maximiliano A. Iramain [a], Lilian Davies [b], Silvia Antonia Brandán [a, *]

[a] Cátedra de Química General, Instituto de Química Inorgánica, Facultad de Bioquímica, Química y Farmacia, Universidad Nacional de Tucumán, Ayacucho 471, 4000, San Miguel de Tucumán, Tucumán, Argentina
[b] Instituto de Investigaciones para la Industria Química (INIQUI, CONICET), Universidad Nacional de Salta, Av. Bolivia 5150, 4400, Salta, Argentina

ARTICLE INFO

Article history:
Received 8 August 2017
Received in revised form
22 September 2017
Accepted 15 January 2018

Keywords:
Potassium 3-furoyltrifluoroborate salt
Vibrational spectra
Molecular structure
Force field
DFT calculations

ABSTRACT

The potassium 3-furoyltrifluoroborate salt has been experimentally characterized by means of FT-IR, FT-Raman and UV–Visible spectroscopies. Here, the predicted FT-IR, FT-Raman and UV–visible spectra by using theoretical B3LYP/6-31G* and 6-311++G** calculations show very good correlations with the corresponding experimental ones. The solvation energies were predicted by using both levels of calculations. The NBO analyses reveal the high stability of the salt by using the B3LYP/6-31G* level of theory while the AIM studies evidence the ionic characteristics of the salt in both media. The strong blue colour observed on the K atom by using the molecular electrostatic potential mapped suggests that this region act as typical electrophilic site. The gap values have revealed that the salt in gas phase is more reactive than in solution, as was reported in the literature while, the F13···H6 interaction together with the K–O bond observed by the studies of their charges could probably modulate the reactivities of this salt in aqueous solution. The force fields were computed with the SQMFF methodology and the Molvib program to perform the complete vibrational analysis. Then, the 39 vibration normal modes classified as 26 A'+ 13 A″ were completely assigned and their force constants are also reported.

1. Introduction

Heteroaryl compounds containing different rings in their structures have very diverse properties according to their nature, number and different substituent groups to which they are attached. Thus, these derivatives are used in numerous syntheses, as intermediates and/or end products and are widely studied from different points of view. In particular, organometallic reagents are of interest in synthetic organic chemistry because they provide conjugation reactions by generating a new approach to the synthesis of conjugated molecules such as protein-proteins and protein-polymer [1–7]. On the other hand, the incorporation of F atoms in their structures makes these compounds can be used mainly in the pharmaceutical industry because they allow their rapid incorporation into the human body. Structural changes obviously produce changes in their properties that are of interest for the design of new drugs with fewer side effects. Here, we propose the study of the potassium 3-furoyltrifluoroborate salt, with molecular formula: $C_5H_3O_2(BF_3K)$, because their structural, electronic, topological and vibrational properties were not reported yet and their crystalline and molecular structure was not experimentally determined and only their synthesis and characterizations by using NMR and mass spectroscopies were recently published [3–7]. The chemical properties of this salt are of importance due to that many studies suggest that there are steric and conformational factors that modulate the reactivities of these salts especially in aqueous solution [3–7]. Thus, in this medium, it was observed that in the amide formation with hydroxyl amines, there is considerable dependence on reactivity depending on the structure of the ligand [3]. Hence, the study of the nature of the different bonds and their interactions are important taking into account those experimental observations. As in the powerful laxative sodium picosulphate [8], possibly the ionic interactions in the potassium furoyltrifluoroborate salt play an important role in their structure and in their biological properties. Thus, the purposes of this work are the structural, electronic, topological and spectroscopic study of this salt in gas phase and in aqueous solution combining DFT calculations with their experimental infrared (FTIR), Raman and electronic spectra. Here, the knowledge of the coordination modes of the B

* Corresponding author.
E-mail address: sbrandan@fbqf.unt.edu.ar (S.A. Brandán).

https://doi.org/10.1016/j.molstruc.2018.01.040
0022-2860/

atoms with the three electronegative F atoms linked to the K atom is very important to understand the mechanisms of all reactions where this salt is involved. These studies were performed by using the hybrid B3LYP method with the 6-31G* and 6-311++G** basis sets in gas phase and aqueous solution [9,10]. Especially in solution, the self consistent force field (SCRF) calculations were performed considering the integral equation formalism variant polarised continuum model (IEFPCM) to analyze the solvent effects [11,12] while the solvation model was used to predict the solvation energies with both levels of theory [13]. Also, the scaled mechanical force field (SQMFF) approach [14] was employed to perform the complete assignments of their vibrational spectra while to predict the reactivities and the behaviors of the salt in both media the frontier orbitals [15,16] and some useful descriptors were also computed [17–21]. Here, the obtained values were compared with data reported in the literature for halogenated compounds with different biological properties [17–21].

2. Experimental

The infrared spectrum of the pure potassium 3-furoyltrifluoroborate salt (FTFB) in solid state was recorded in KBr pellets on a Perkin Elmer Spectrum GX spectrometer in the 4000 to 400 cm^{-1} range. The Raman spectrum of FTFB in solid state at room temperature was recorded between 3600 and 100 cm^{-1} with the optical module of the Perkin Elmer Spectrum GX Raman equipped with an yttrium aluminum garnet crystal doped with triply-ionized neodymium laser (excitation line of 1064 nm, 1900 mW of laser power). The Raman spectrum was recorded with 100 scans and a resolution of 4 cm^{-1}. The ultraviolet spectrum was recorded in aqueous solution with a Beckman spectrophotometer between 200 and 800 nm.

3. Computational details

The potassium 3-furoyltrifluoroborate salt was easily modeled with the *GaussView* program [22] because it salt structurally has a furane ring linked to the trifluoroborate group (BF_3K). Then, this initial structure was optimized in gas phase by using the hybrid B3LYP and the two 6-31G* and 6-311++G** levels of theory [9,10] with the Gaussian 09 program [23]. Later, with these optimized structures were performed the potential energy surfaces (PES) considering the three dihedral C1–C2–C9–O10, C2–C9–B11–K15 and F13–B11–C9–O10 angles and both levels of theory. The two first curves mentioned are presented in Fig. 1. In each curve we observed two stable structures with the same energies, named in the first case C1 and C2, while in the other one C3 and C4 where one of them, C4 presents the lowest energy. Hence, it is easy to see that C4 is the most stable structure of FTFB which can be seen in Fig. 2. When the F13–B11–C9–O10 dihedral angle is also considered two stable structures were obtained which correspond to C2 and C4 and, for this reason, this curve was not presented here. In solution, these stable structures were optimized with the PCM/SMD models [11–13] and the Gaussian 09 program [23]. In this opportunity the atomic Mulliken and natural populations (NPA) charges were studied with both basis sets and in the two media. The NBO program [24] was used to calculate the bond orders, expressed as Wiberg indexes and the donor-acceptor interactions while the AIM2000 program was used to compute the topological properties [25]. To perform the vibrational analysis of FTFB in both media, their normal internal coordinates, the SQMFF approach [14] and the Molvib program [26] were employed to calculate the force fields with both levels of theory. The normal internal coordinates corresponding to the BF_3K group were building taking into account a C_{3v} symmetry, as in species with similar groups [8,17–19,21] while the

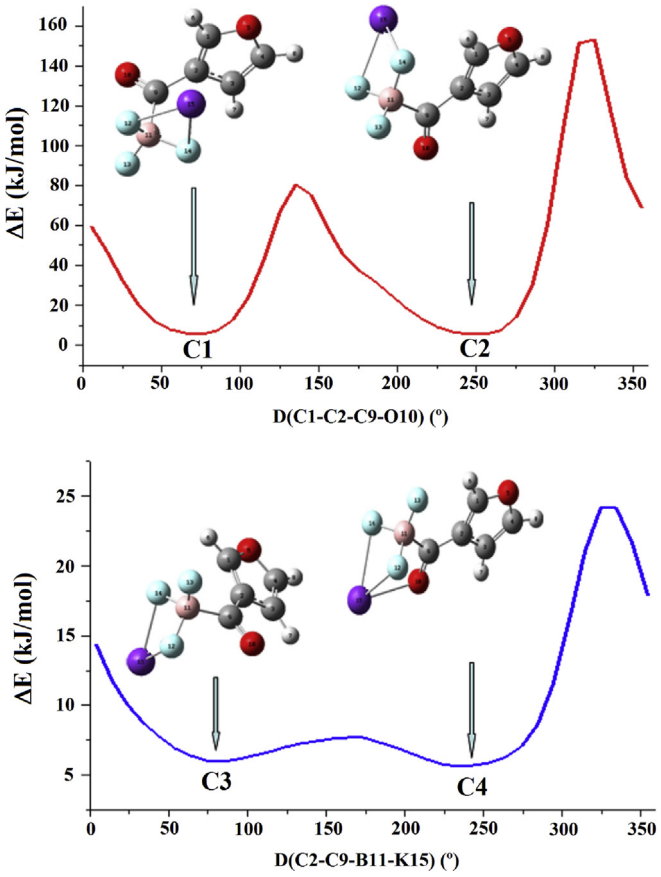

Fig. 1. Potential energy surfaces (PES) described by the dihedral C1–C2–C9–O10 (Top) and C2–C9–B11–K15 (Bottom) angles for the potassium 3-furoyltrifluoroborate salt in gas phase by using the B3LYP/6-31G* level of theory.

C4 structure was optimized with C_s symmetry. The assignments of all vibration modes were performed using the potential energy distribution (PED) contribution ≥ 10%. In addition, the ultraviolet–visible spectrum of FTFB in water was predicted by using Time-dependent DFT calculations (TD-DFT) with both levels of theory and the Gaussian 09 program [23]. Finally, taking into account that steric and conformational factors could modulate the

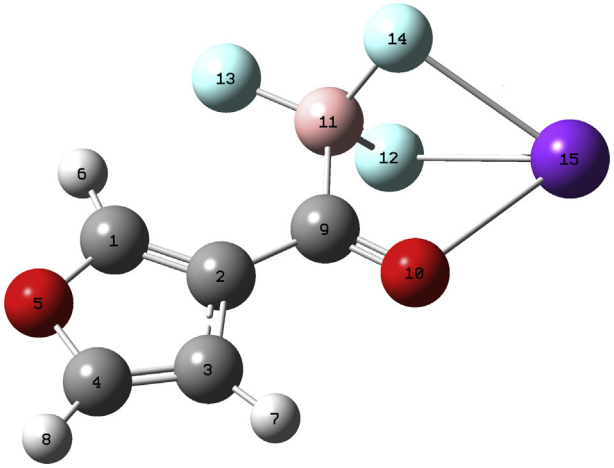

Fig. 2. Molecular structure of the most stable C4 conformer of the potassium 3-furoyltrifluoroborate salt and atoms numbering.

reactivities of these salts especially in aqueous solution [3–7] we have calculated the frontier orbitals for FTFB in both media in order to predict their reactivities and behaviours by using the chemical potential (μ), electronegativity (χ), global hardness (η), global softness (S), global electrophilicity index (ω) and nucleophilicity indexes (E) descriptors [17–21] which were posterior compared with other substances with different biological properties [27–30].

4. Results and discussion

4.1. Structural study in gas phase and in aqueous solution

Table 1 shows the properties calculated for FTFB in gas and aqueous solution phases by using both levels of theory. Hence, the total and relative energies, dipolar moments molecular volume and volume variations together with their populations and dihedral angles for the different structures can be seen in Table 1. The results show clearly that the C4 structure has the lower energy values by using both methods for which it is the most stable conformer of FTFB in both media. Thus, C4 contain the major populations and low dipole moment values in the two media and, where these values increase slightly in solution with both basis sets. Fig. 2 shows the optimized C4 structure by using the B3LYP/6-31G* level of theory. Hence, obviously we have considered only C4 to analyze all properties in gas phase. The dipole moment vector for C4 of FTFB in gas phase is given in Fig. S1 where we can see that the direction of this vector is clearly oriented from the F atoms toward the K atom. The Moldraw program [31] was used to compute the volume values for all conformers in both media, later, the differences observed between the values in gas phase in relation to the values in solution are calculated as volume variations. Note that the values of the dihedral C1–C2–C9–O10, C2–C9–B11–K15 and F13–B11–C9–O10 angles in C4 are respectively, 180, 180 and 0°. These results

Table 2
Calculated solvation energies (ΔG) for the most stable C4 conformer of the 3-furoyltrifluoroborate salt by using the B3LYP/6-31G* and B3LYP/6-311++G** methods.

Solvation energies (kJ/mol)			
METHOD	$\Delta G_u^{\#}$	ΔG_{ne}	ΔG_c
B3LYP/6-31G*	−51.93	23.86	−75.79
B3LYP/6-311++G**	−58.23	23.32	−81.55

$\Delta G_u^{\#}$, uncorrected; ΔG_{ne}, non electrostatic terms; ΔG_c, corrected.

can be observed in Table 1 where the C4 conformer presents volume expansion having the lowest volume variation in solution (1.5 and 1.7 Å^3 by using the 6-31G* and 6-311++G** basis sets, respectively) with solvation energy values of −75.79 and −81.55 kJ/mol, by using the 6-31G* and 6-311++G** basis sets, respectively, as indicated in Table 2. If these values are compared with those obtained for the picosulphate salt [8] (solvation energy value of −254.38 kJ/mol and volume variation of 13.3 Å^3), here, probably their high dipole moment value of 15.14 D in solution could explain the great difference observed between both salts due to their major hydration. Here, the solvation energy value due to the non electrostatic terms were calculated from the PCM calculations [11,12] by using the Solvation model [13] while the uncorrected values were computed from the difference between the energy values in solution than the corresponding in gas phase.

The FTFB structure was not experimentally determined and, for this reason, the geometrical parameters for C4 were compared with those reported in the literature for 4-methylbenzoylboronate (E)-1-(((4-Bromophenyl)imino)methyl)naphthalen-2-o [32], 4-methylbenzoylboronate(E)-2-(((2-(Hydroxymethyl)phenyl)imino)methyl)phenol [33] and the furonic acid [34] by using the root-mean-square deviation (RMSD) values which can be seen in bold

Table 1
Calculated total (E) and relative energies (ΔE), dipole moments, molecular volume and volume variations (ΔV) and populations (%) for the 3-furoyltrifluoroborate salt.

B3LYP/6-31G*method									
GAS PHASE									
Conformers	E (Hartrees)	μ (Debye)	V (Å^3)	ΔE (KJ/mol)	ΔV (Å^3)	Population (%)	Dihedral angles (°) C1C2C9O10	C2C9B11K15	F13B11C9O10
C1	−1267.2621	11.85	225.2	70.03		0	72.3	44.1	48.6
C2	−1267.2636	11.39	224.9	66.10		0	−165.4	44.1	48.6
C3	−1267.2788	8.61	228.4	26.22		0	179.9	−179.9	−179.9
C4	−1267.2888	7.61	228.4	0.00		100	180.0	180.0	0.0
AQUEOUS SOLUTION/PCM									
C1	−1267.2966	16.0	221.0	31.48	−4.2	0	25.8	28.5	32.9
C2	−1267.2997	15.72	233.6	20.33	8.7	0	−173.2	−142.3	41.4
C3	−1267.2998	14.23	234.0	23.08	5.6	0	176.1	87.1	82.4
C4	−1267.3086	8.78	229.9	0.00	1.5	100	180.0	180.0	0.0
B3LYP/6-311++G**method									
GAS PHASE									
Conformers	E (Hartrees)	μ (Debye)	V (Å^3)	ΔE (KJ/mol)	ΔV (Å^3)	Population (%)	Dihedral angles (°) C1C2C9O10	C2C9B11K15	F13B11C9O10
C1	−1267.5075	11.42	227.2	67.44		0	33.0	24.3	28.7
C2	−1267.5148	12.19	226.0	64.74		0	−160.2	36.0	39.4
C3	−1267.5294	7.79	223.9	26.22		0	−179.9	−179.9	179.9
C4	−1267.5394	7.79	229.0	0.0		100	180.0	180.0	0.0
AQUEOUS SOLUTION/PCM									
C1	−1267.5512	17.51	218.9	272.8	−8.3	0	31.6	20.9	23.0
C2	−1267.5522	19.21	237.8	24.67	13.9	0	−176.0	59.4	125.2
C3	−1267.5562	12.69	227.8	14.16	3.9	0	178.5	122.2	122.8
C4	−1267.5616	9.20	230.7	0.00	1.7	100	180.0	180.0	0.0

Table 3
Comparison of calculated geometrical parameters for the 3-furoyltrifluoroborate salt.

B3LYP method[a]					Experimental		
Parameters	6-31G*		6-311++G**		EXP[b]	EXP[c]	EXP[d]
	Gas	PCM	Gas	PCM			
Bond lengths (Å)							
C1–C2	1.373	1.373	1.371	1.371	1.391	1.402	1.345
C2–C3	1.444	1.447	1.444	1.447	1.487	1.398	1.411
C3–C4	1.353	1.352	1.350	1.348	1.382	1.393	1.339
C4–O5	1.376	1.387	1.375	1.387			1.359
C1–O5	1.351	1.356	1.349	1.353			1.366
C1–H6	1.077	1.078	1.076	1.076			
C4–H8	1.079	1.079	1.076	1.077			
C3–H7	1.080	1.080	1.077	1.078			
C2–C9	1.466	1.463	1.463	1.459	1.487	1.497	1.456
C9=O10	1.253	1.254	1.247	1.249	1.225	1.235	1.255
C9–B11	1.650	1.642	1.649	1.641	1.635	1.646	
B11–F12	1.437	1.429	1.446	1.439			
B11–F13	1.380	1.393	1.382	1.400	1.384	1.389	
B11–F14	1.438	1.429	1.446	1.439			
K15–F14	2.555	2.662	2.585	2.727			
K15–F12	2.557	2.660	2.584	2.726			
K15–B11	2.930	3.036	2.973				
K15–O10	2.597	2.684	2.595	2.676			
RMSD[b]	**0.025**	**0.025**	**0.025**	**0.026**			
RMSD[c]	**0.029**	**0.030**	**0.030**	**0.032**			
RMSD[d]	**0.020**	**0.021**	**0.019**	**0.020**			
Bond angles (°)							
C1–C2–C3	105.5	105.7	105.6	105.8	119.2	118.8	106.3
C2–C3–C4	106.2	106.5	106.2	106.5	120.8	120.5	106.3
C3–C4–O5	110.4	110.2	110.3	110.0			110.8
C4–O5–C1	106.9	106.9	107.1	107.1			105.7
O5–C1–C2	110.7	110.5	110.5	110.4			110.5
O5–C1–H6	116.9	116.1	117.0	116.2			
C2–C1–H6	132.3	133.2	132.4	133.3			
C2–C3–H7	126.0	126.5	126.2	126.8			
C4–C3–H7	127.6	126.8	127.4	126.6			
C3–C4–H8	134.3	134.6	134.1	134.5			
O5–C4–H8	115.1	115.1	115.4	115.4			
C1–C2–C9	126.8	126.8	126.9	126.8	119.2	120.2	131.9
C3–C2–C9	127.5	127.4	127.4	127.2			
C2–C9–O10	117.9	118.2	118.5	118.9	117.9	118.3	117.3
C2–C9–B11	123.2	123.9	123.7	124.6			
O10–C9–B11	118.7	117.8	117.6	116.4	116.7	121.2	
C9–B11–F14	106.7	107.5	106.8	107.8			
C9–B11–F13	115.0	114.9	116.0	116.3	116.4	113.1	
C9–B11–F12	106.7	107.5	106.8	107.8			
F14–K15–F12	53.2	50.9	52.5	49.6			
F14–K15–B11	29.3	28.0	29.1	27.5			
F14–K15–O10	69.1	66.1	68.1	64.8			
B11–K15–F12	29.3	28.0	29.1	27.5			
B11–K15–O10	53.5	28.0	52.5	49.7			
F12–K15–O10	69.0	66.1	68.1	64.8			
RMSD[b]	**8.8**	**8.6**	**8.7**	**8.6**			
RMSD[c]	**8.5**	**8.4**	**8.6**	**8.6**			
RMSD[d]	**2.0**	**2.0**	**2.0**	**2.1**			
Dihedral angles (°)							
O10–C9–B11–F14	−56.2	−57.0	−55.8	−56.7			
O10–C9–B11–F13	−179.9	57.0	179.9	179.9	166.9	−113.2	
O10–C9–B11–F12	56.2	57.0	55.7	56.6			
C2–C9–B11–F14	123.7	122.8	124.2	123.2			
C2–C9–B11–F13	0.04	−0.00	−0.04	−0.04	−14.4	69.1	
C2–C9–B11–F12	−123.6	−124.2	−122.9	−123.3			
C1–C2–C9–B11	−0.03	0.01	0.00	−0.01			
C3–C2–C9–B11	179.9	179.9	−179.9	179.9			
C1–C2–C9–O10	179.9	−179.9	179.9	179.9			
C3–C2–C9–O10	−0.02	−0.01	−179.9	−0.01			
RMSD[b]	**245.4**	**78.4**	**13.7**	**13.7**			
RMSD[c]	**67.9**	**129.9**	**212.9**	**212.9**			

[a] This work.
[b] From Ref [32].
[c] From Ref [33].
[d] From Ref [34].

letters in Table 3. It is necessary to clarify that the most stable C4 structure was optimized with C_s symmetry, where the B11 and K17 atoms are in the same plane than the furane ring and, where the B atom has coordination five, as also was observed in the $K_5[B(SO_4)_4]$ salt [17] while the K atom present coordination four, as can be seen in Fig. 2. In Fig. S2 we can see the common part compared among those three structures by using circles. Here, we can clearly see that the better correlations for bond lengths and angles (between 0.019 and 0.021 Å and 2.1–2.0°) are obtained when the values for both basis sets are compared with the furonic acid [34]. In relation to the dihedral angles only for two experimental values from Refs. [32] and [33] can be compared where, in the first case the correlation is very bad for FTFB in gas phase while notably improve when their values are compared with that experimental obtained from Ref. [33]. Here, Table 3 shows that when increase the size of the basis set we observed that decrease the bond lengths while for a same basis set the values slightly increase in solution.

4.2. NPA and Mulliken charges, MEP and bond orders

For FTFB, we investigate two charge's types because it is very important to know the characteristic of the different bonds present in both media and by using the two basis sets. Hence, the Mulliken and atomic natural population charges values are presented in Table S1 while their comparisons in gas phase by using B3LYP/6-31G* method are represented in Fig. S3 because it is easy to see graphically the positive and negative values and their differences. Thus, both charges predicted negative values on the C2, C3, O5, O10, F12, F13 and F14 atoms, where clearly the more negative values are observed on the O10, F12 and F14 atoms, having the O10 atom the lowest value. On the other hand, the more positive values are observed on the C1 and C4 atoms, on all H atoms, and on the B11 and K15 atoms, presenting the higher value the B11 atom. Note that the Mulliken charges predicted lower values on all atoms than the corresponding to the NPA ones. The changes in the values of the two charges and in both media can be observed in Fig. S4. Few changes are observed in the NPA charges in both media and by using the two basis sets while the Mulliken charges values are most negative on the O10 atoms in relation to the other negative atoms. The NPA charges in both media with the 6-311++G** basis set show the proximities in the values on the O10 atoms with those observed on the three F atoms while the Mulliken charges with this basis set show great differences among them including positive values are observed on the C2 and C3 atoms while on the C1 atoms in both media are observed negative values.

The studies of the nucleophilic and electrophilic regions are of great importance in this salt with potential pharmacological properties because it presents strong electronegative and electropositive atoms, such as are the F and K atoms, respectively. Hence, two different positions corresponding to the molecular electrostatic potential surface mapped for FTFB in gas phase by using the B3LYP/6-31G* method are presented in Fig. S5. These figures show on the F and O atoms slight red colours indicating that these are nucleophilic sites while on the K atoms strong blue colours can be observed typical of electrophilic sites. These regions are important reaction sites that confer to FTFB a higher electrophilic character, as revealed by their surfaces mapped.

The bond order (BO) expressed as Wiberg indexes were calculated for FTFB in both media and by using the two methods in order to analyze the characteristics of the different bonds and to verify the different coordination numbers predicted for the F and B atoms. The values can be seen in Table S2 including the values for some bonds taken from the bond order matrix while their behaviours in both media by using 6-31G* basis set are represented in Fig. S6. The results show that the B atoms in both media and by using the two methods have coordination number five while the K atoms present coordination number four. On the other hand, analyzing exhaustively the graphic we observed that the C atoms belong to the ring present the higher values, as expected because they have double bond characters while the lower values are observed for all the H atoms having the lowest values the K atoms in both media. Note that practically there are not observed changes in solution. Here, the low values observed for the K atoms of 0.099 in gas phase and of 0.064 in solution by using the 6-311++G** basis set show clearly their ionic characteristics. When the other basis set is used a same behaviour it is observed in both media.

4.3. Stability studies by using NBO and AIM calculation

The stability of this salt was investigated in both media by using the contributions energetically observed with the NBO calculations [20] and from the intra-molecular interactions with the Bader's theory of atoms in molecules (AIM) [35] by using the AIM2000 program [25]. The donor-acceptor energy interactions in both media and by using the two 6-31G* and 6-311++G** basis sets are shown in Table S3. The analysis of these results show that: (i) with the 6-31G* basis set in both media only three interactions are observed which are the $\Delta E_{\pi\rightarrow\pi^*}$, $\Delta E_{n\rightarrow\pi^*}$ and $\Delta E_{n\rightarrow\sigma^*}$ interactions, where the more important are those located from the lone pairs corresponding to the O and F atoms toward the anti-bonding C–C, C–B and B–F orbitals, (ii) for FTFB in both media with the 6-311++G** levels of theory only are observed the $\Delta E_{\pi\rightarrow\pi^*}$ and $\Delta E_{n\rightarrow\sigma^*}$ interactions and, finally, (iii) the higher contributions to the total energies are observed for the 6-31G* basis set. Here, in this study we observed clearly the influence of the size of the basis set on the total energies. The 6-311++G** basis set decrease notably the energy values in both media.

The topological properties are essential parameters to investigate the different interactions existent in a molecule, as reported by Bader [35]. In particular, the presence of both electropositive and electronegative atoms in the potassium 3-furoyltrifluoroborate salt probably generates ionic or H bonds interactions which could confer important properties to this salt. For these reasons, the AIM2000 program [25] was used to calculate, in accordance with the Bader's theory, the electron density distribution, $\rho(r)$ and the Laplacian values, $\nabla^2\rho(r)$ together with the eigenvalues ($\lambda 1$, $\lambda 2$, $\lambda 3$) of the Hessian matrix and the $\lambda 1/\lambda 3$ ratio in the bond critical points (BCPs). These parameters calculated for both basis sets and in both media can be seen in Table S4. Here, the values observed of $\lambda 1/\lambda 3 < 1$ and $\nabla^2\rho(r) > 0$ in the BCPs and ring critical points (RCPs) predicted in both media by using the 6-31G* basis set a intra-molecular F bond and three ionic interactions which are respectively, F13–H6, F14–K15, K15–F12 and K15–O10 where the latter interaction present the more high densities. These are named closed-shell interactions and the details of the molecular model for FTFB in gas phase by using 6-31G* basis set can be seen in Fig. S7. Here, possibly the different electronegativities of both K15 and O10 atoms clearly justify that observation despite the distances between both atoms are higher than the other ones (2.597 Å in gas phase). When the topological parameters calculated in both media with the 6-31G* basis set are compared with those calculated by using the 6-311++G** basis set we observed that the F13–H6 interactions observed in both media disappear and, besides an increasing in the parameters values it is observed. Here, when the topological properties for all RCPs are compared we observed that, obviously, the furane ring has the higher values in both media and by using the two basis sets, as expected because it is properly a ring of FTFB.

The AIM analyses evidence the high stability of this salt due to the four intra-molecular interactions observed. The ionic nature of this salt is elucidated by the AIM analysis.

4.4. Frontier orbitals and descriptors

The prediction of reactivities and the behaviours of the FTFB salt is the great importance taking into account the different studies reported for this salt where suggest that there are steric and conformational factors that modulate the reactivities of these salts especially in aqueous solution [3–7]. Thus, the frontier orbitals in both media and with the two basis sets were calculated to compute the gap values [15,16] and with these gap values were later calculated the chemical potential, electronegativity (χ), global hardness (η), global softness (S), global electrophilicity index (ω) and global nucleophilicity index (E) [19–21,27–30]. All parameters can be seen in Table S5 compared with those reported for the sodium picosulfate salt [8] and for the thiol tautomer of 1,3-benzothiazole [30] because these compounds have laxative and antimicrobial activity in aqueous solution, respectively. Very interesting results are obtained when the gap values are first analyzed for FTFB in both media. Thus, we observed that FTFB in gas phase is more reactive than in solution and, that by using the 6-31G* basis set the reactivity increase. Hence, effectively as reported by those experimental results the salt is less reactive in solution. A possible explanation could be justified by the following studies. Probably, the decreasing in the BO value observed for the F13 atom in solution with both basis sets is due to increasing in the Mulliken and NPA charges on this atom. Besides, both charges on the K atoms increase in solution for which increase the BO of the O10 atom and, for this reason, the lone pairs on this atom can be easily shared in solution by H bonds formation with water molecules. This way, the F13···H6 interaction together with the K–O bond observed for this salt could probably modulate their reactivities in aqueous solution.

On the other hand, when the gap values for FTFB are compared with the laxative sodium picosulfate [8] and with the antimicrobial thiol 1,3-benzothiazole [30] (Fig. S8) we observed that both are more reactive than FTFB but picosulfate is most reactive probably because this salt has three rings, two sulfate groups and two sodium atoms in their structure while that the thiol tautomer has only two rings and the S–H group. Evidently, the presences of these different groups increase the reactivities of these compounds. When the descriptors are first compared for FTFB we observed that in solution increase the nucleophilicity (E) with both basis sets, then, it implies that FTFB has most capability of H bonds formation, as above was explained while the electrophilicity decrease by using the 6-31G*basis set but increase in solution with the other one. Thus, there is not a defined tendency. Fig. S9 shows proximity among the descriptors of all compared species where the differences are clearly observed in the nucleophilicity and electrophilicity values showing the thiol tautomer the most different values. These results also could explain why the reactivity of the FTFB salt is modulated in solution.

4.5. Vibrational analysis

The potassium 3-furoyltrifluoroborate salt was optimized with C_s symmetry in both media and by using both basis sets, hence, 39 vibration normal modes active in both IR and Raman spectra are expected for this salt. These modes are classified as, 26 A'+ 13 A″ where the A′ modes are planar while the A″ are out-of-plane. The experimental IR and Raman spectra of FTFB in the solid state are given in Figs. 3 and 4, respectively which are compared with the corresponding predicted in gas phase by using the two basis sets. Very good correlations are observed among the experimental and theoretical IR and Raman spectra. Obviously, the transformation of both Raman spectra from scattering activities to intensities by means of well-known equations [36,37] generate, better

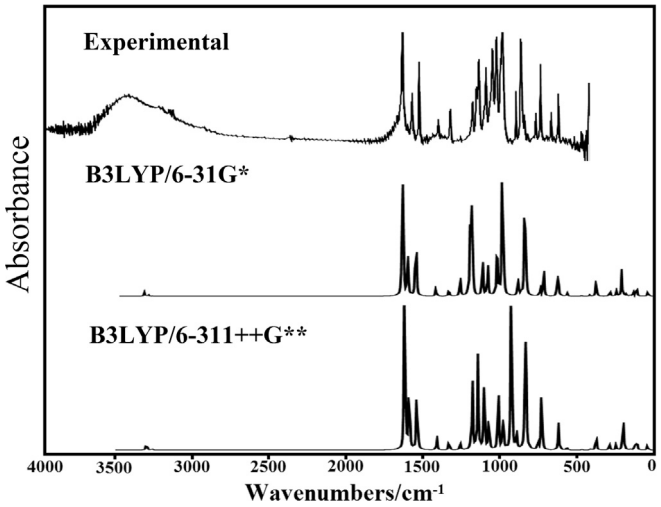

Fig. 3. Experimental infrared in the solid state of the potassium 3-furoyltrifluoroborate salt compared with the corresponding predicted for the C4 conformer by using B3LYP/6-31G* and B3LYP/6-311++G** levels of theory.

correlations in the bands, as can be seen in Fig. 4. The observed and calculated wavenumbers together with the assignments for the most stable C4 conformer of the salt by using both methods and, in the two studied media are presented in Table 4. Modifications in the assignments are observed principally with the increase in the size of the basis set that when the medium change of gas phase to solution. The complete vibrational analyses with their corresponding assignments were performed by using the SQMFF approach [14], the internal normal coordinates and the Molvib program [26]. Observed and calculated wavenumbers, potential energy distributions and assignment for the most stable conformer for the potassium 3-furoyltrifluoroborate salt in both media by using the two methods can be seen in Tables S6–S9. In this work, the normal internal coordinates were not presented because they

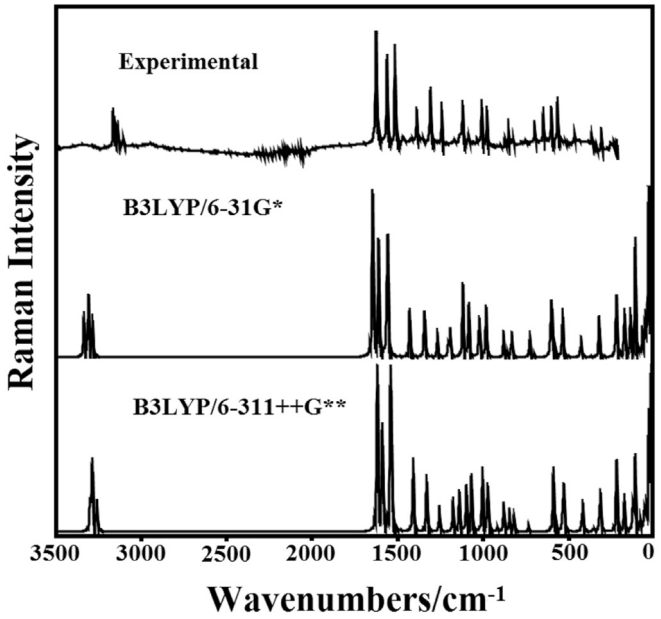

Fig. 4. Experimental Raman in the solid state of the potassium 3-furoyltrifluoroborate salt compared with the corresponding predicted for the C4 conformer by using B3LYP/6-31G* and B3LYP/6-311++G** levels of theory.

Table 4
Observed and calculated wavenumbers (cm^{-1}) and assignments for the most stable C4 conformer of the potassium 3-furoyltrifluoroborate salt in gas and aqueous solution phases.

Experimental			B3LYP 6-31G*[a]				B3LYP 6-311++G**[a]			
			Gas		PCM		Gas		PCM	
Modes	IR	Raman	SQM[b]	Assignment[a]	SQM[b]	Assignment[a]	SQM[b]	Assignment[a]	SQM[b]	Assignment[a]
A′ Symmetry										
1	3160w	3161vw	3195	νC1–H6	3195	νC1–H6	3158	νC1–H6	3157	νC1–H6
2	3151w	3151vw	3170	νC4–H8	3178	νC4–H8	3147	νC4–H8	3150	νC4–H8
3	3134w	3133vw	3146	νC3–H7	3147	νC3–H7	3123	νC3–H7	3121	νC3–H7
4	1622vs	1623vs	1582	νC9=O10	1561	νC9=O10	1556	νC9=O10	1536	νC1–C2
5		1559s	1553	νC1–C2	1549	νC3–C4	1532	νC1–C2	1520	νC9=O10
6	1512m	1513vs	1502	νC3–C4	1497	νC1–C2	1484	νC3–C4	1477	νC3–C4
7		1385m	1383	νC2–C3	1380	νC2–C3	1366	νC2–C3	1363	νC2–C3
8	1306w	1304s	1299	νC2–C9	1295	νC2–C9	1287	νC2–C9	1282	νC2–C9
9		1238m	1235	βC1–H6	1234	βC1–H6	1224	βC1–H6	1225	βC1–H6
10	1159m	1163w	1163	ν_aBF_3	1129	νC1–O5	1139	νC1–O5	1109	βC3–H7
11	1133m	1116m	1159	νC1–O5	1105	ν_aBF_3	1111	ν_aBF_3	1062	νC1–O5
12	1071m	1081w	1090	βC4–H8	1076	βC4–H8	1070	βC4–H8	1030	βC4–H8
13	1028s	1031w	1052	νC4–O5	1039	βC3–H7	1035	νC4–O5	1011	ν_aBF_3
14	1002s	1004m	994	βC3–H7	984	νC4–O5	978	βC3–H7	967	νC4–O5
15	964s	967sh	967	βR_2	959	βR_2	904	ν_aBF_3	888	ν_aBF_3
16	873m	869w	879	βR_1	871	βR_1	880	βR_1	873	γC3–H7
17	841s	848m	832	γC1–H6	833	γC1–H6	845	γC1–H6	845	γC1–H6
18	641w	644m	617	δ_sBF_3	615	δ_sBF_3	603	δ_sBF_3	598	δ_sBF_3
19	594m	561s	560	δB11C9C2	557	βC2–C9	554	δB11C9C2	550	βC2–C9
20	461vw	461m	467	δ_aBF_3	463	δ_aBF_3	459	δ_a BF_3	452	δ_aBF_3
21	393m	360m	373	βC9=O10	363	βC9=O10	368	βC9=O10	358	βC9=O10
22		304m	282	νC9–B11	284	νC9–B11	280	νC9–B11	280	νC9–B11
23		250m	244	ρBF_3	239	ρBF_3	243	ρBF_3	236	$\rho' BF_3$
24		190sh	202	νF14–K15	165	νF14–K15	190	νF14–K15	162	γC2–C9
25		153vw	157	δK15B11C9	149	δB11C9C2	150	δK15B11C9	136	δB11C9C2
26		111vw	114	βC2–C9	92	δK15B11C9	108	βC2–C9	77	νF14–K15
A″ Symmetry										
27	975s	974m	969	ν_aBF_3	968	ν_aBF_3	959	βR_2	948	βR_2
28		863w	860	γC3–H7	864	γC3–H7	873	γC3–H7	871	βR_1
29	818w	819w	829	ν_sBF_3	821	ν_sBF_3	815	ν_sBF_3	802	ν_sBF_3
30	796vw	773w	734	γC4–H8	733	γC4–H8	741	γC4–H8	733	γC4–H8
31	712m	694m	707	γC9=O10	708	γC9=O10	712	γC9=O10	709	γC9=O10
32		597w	603	τR_1	592	τR_1	597	τR_2	583	τR_1
33		590sh	590	τR_2	583	τR_2	585	τR_1	578	τR_2
34	414vw	418w	414	δ_aBF_3	417	δ_aBF_3	403	δ_aBF_3	405	δ_aBF_3
35		238m	238	$\rho' BF_3$	232	$\rho' BF_3$	242	$\rho' BF_3$	234	ρBF_3
36		175vw	174	γC2–C9	162	γC2–C9	175	γC2–C9	148	νF12–K15
37		120vw	130	νF12–K15	100	νF12–K15	117	νF12–K15	88	δK15B11C9
38			69	τwC2–C9	55	τwC2–C9	66	τwC2–C9	40	τwC2–C9
39			37	τwBF_3	30	τwBF_3	37	τwBF_3	21	τwBF_3

Abbreviations: ν, stretching; β, deformation in the plane; γ, deformation out of plane; wag, wagging; τ , torsion; β_R, deformation ring τ_R, torsion ring; ρ,rocking; τw, twisting; δ, deformation; a, antisymmetric; s, symmetric.
[a] This work.
[b] From scaled quantum mechanics force field.

are in accordance with those reported for compounds with similar ring [18–21,27–30]. The force fields were calculated with both methods and levels of theory and considering the potential energy distribution (PED) contributions ≥ 10%. The assignments for some groups are briefly discussed below.

4.5.1. Band assignments

4.5.1.1. CH modes. For FTFB, only three C1–H6, C3–H7 and C4–H8 stretching modes are expected which are predicted by the two levels of theory and in both media with A′ symmetries and between 3195 and 3121 cm^{-1}. Hence, these modes are easily assigned to the IR and Raman bands observed between 3161 and 3133 cm^{-1}. The in-plane deformation or rocking modes are predicted in different regions by using both methods and with A′ symmetries, thus, the IR and Raman bands between 1238 and 1002 cm^{-1} can be clearly assigned to these vibration modes. Two out-of-phase modes are predicted with A″ symmetries between 873 and 733 cm^{-1} while the other one with A′ symmetry around 845 cm^{-1}, hence; these modes are assigned to the IR and Raman observed in these regions, as indicated in Table 4.

4.5.1.2. BF_3 modes. These modes by using the two methods are predicted in different regions and with different symmetries. Thus, the SQM/B3LYP/6-31G* calculations predicted only one of the two antisymmetric stretching modes with A′ symmetry at 1163 cm^{-1} in gas phase and at 1105 cm^{-1} in solution while the other antisymmetric and symmetric stretching modes are predicted with A″ symmetries between 969 and 821 cm^{-1}, as detailed in Table 4. On the other hand, the SQM/B3LYP/6-311++G** calculations predicted the two antisymmetric stretching modes with A′ symmetries at 1111 and 888 cm^{-1} while the symmetric stretching modes in both media are predicted with A″ symmetries at 815 and 802 cm^{-1}. For these reasons, these stretching modes are assigned to the IR and Raman bands in these regions, as predicted by the calculations. In relation to the antisymmetric and symmetric deformation modes expected for these groups, both levels of calculations predicted one

antisymmetric mode and the corresponding symmetric mode with A′ symmetries between 617/598 and 467/452 cm^{-1} while the other antisymmetric modes are predicted with A″ symmetries between 417 and 403 cm^{-1}. Hence, these modes are assigned as predicted by the SQM calculations and, as indicated in Table 4.

The two expected BF_3 rocking modes were predicted with different symmetries by using both levels of calculations at 244/236 and 242/232 cm^{-1}. Consequently, they were assigned according to the calculations. Both methods predicted the twisting modes for FTFB in the two media with A″ symmetries between 37 and 21 cm^{-1}, hence, these modes could not be assigned because the Raman spectrum was recorded only up to 100 cm^{-1}, as shown in Table 4.

4.5.1.3. Skeletal modes. The C9=O10 stretching modes are easily assigned to the very strong IR band at 1622 cm^{-1} because the two methods predicted these modes with A′ symmetries in gas phase between 1582 and 1556 cm^{-1} while in solution the bands undergoes a shifting toward lower wavenumbers probably due to the hydration of these groups with water molecules. The C1=C2 and C3=C4 stretching modes belong to the furane ring are assigned to the two strong Raman bands at 1559 and 1513 cm^{-1}, as predicted by calculations and as reported for furoic acid [34]. The two F14–K15 and F12–K15 stretching modes are predicted by using the 6-31G* and 6-311++G** basis sets with A′ and A″ symmetries, respectively and, hence, both modes are assigned to the Raman bands and shoulders at 190, 111 and 120 cm^{-1}, respectively. The SQM/B3LYP/6-31G* calculations predicted the two deformation ring modes with A′ symmetries in both media while the expected torsion ring modes are predicted with A″ symmetries. Later, the other method used predict one deformation mode with A′ symmetry and the other one with A″ symmetry while the two torsion modes are predicted with A″ symmetries. Therefore, they were assigned accordingly. In Table 4 is observed the assignments for the remaining skeletal modes which were performed in accordance to the calculations.

5. Force field

In this work, we have calculated the force constants for FTFB because the presence of ionic F–K bonds and of halogen F–H bonds in the different media can also be useful to explain why the steric and conformational factors modulate the reactivities of these salts, in particular in aqueous solution [3–7]. Therefore, the force fields in both media at the 6-31G* and 6-311++G** levels of theory were used to compute the force constants whose values are summarized in Table 5 while in Fig. S10 are graphed their values in the two media and by using both basis set. Obviously, the higher values are observed for the *f(νC=O)* force constants where the value in gas phase calculated by using the 6-31G* basis set is higher than the other ones. Note that the lower force constants values in solution are observed with the B3LYP/6-311++G** method. On the other hand, the *f(νBF$_3$)* force constants computed in both media by using the B3LYP/6-31G* level of theory present the higher values while the *f(νC-O)$_R$* force constant computed to the furane ring in gas phase by using the B3LYP/6-31G* method has the higher value. Hence, it is easy to observe that the size of the basis set produce a decreasing in the force constants values mentioned before but the *f(νC-H)$_R$*, *f(νC-C)$_R$*, and *f(νC-B)* force constants do not change neither with the media nor with the size of the basis set. Here, it is very important to mention that the slight increase observed in the *f(νBF$_3$)* force constant in solution by using only 6-31G* basis set can be easily explained because one of F atoms belong to the BF_3 group present in both media the F–H bond formation due to their C_S structure (see

Table 5
Comparison of scaled internal force constants for the most stable conformer for the potassium 3-furoyltrifluoroborate salt in gas and aqueous solution phases by using two levels of theory.

Force constants	B3LYP/6-31G*[a]		B3LYP/6311++G**[a]	
	Gas	PCM	Gas	PCM
f(νC-H)$_R$	5.49	5.50	5.39	5.39
f(νC-O)$_R$	5.59	5.22	5.41	5.01
f(νC-C)$_R$	6.84	6.83	6.68	6.66
f(νC=O)	10.07	9.77	9.81	9.41
f(νC-B)	2.94	2.97	2.89	2.92
f(νBF$_3$)	4.18	4.12	3.78	3.64
f(δC-C–B)	1.21	1.12	1.12	1.00
f(δBF$_3$)	1.28	1.24	1.24	1.18
f(ρBF$_3$)	1.02	0.98	0.98	0.89

ν, stretching; *δ*, angle deformation.
Units in mdyn Å^{-1} for stretching and mdyn Å rad $^{-2}$ for angle deformations.
[a] This work.

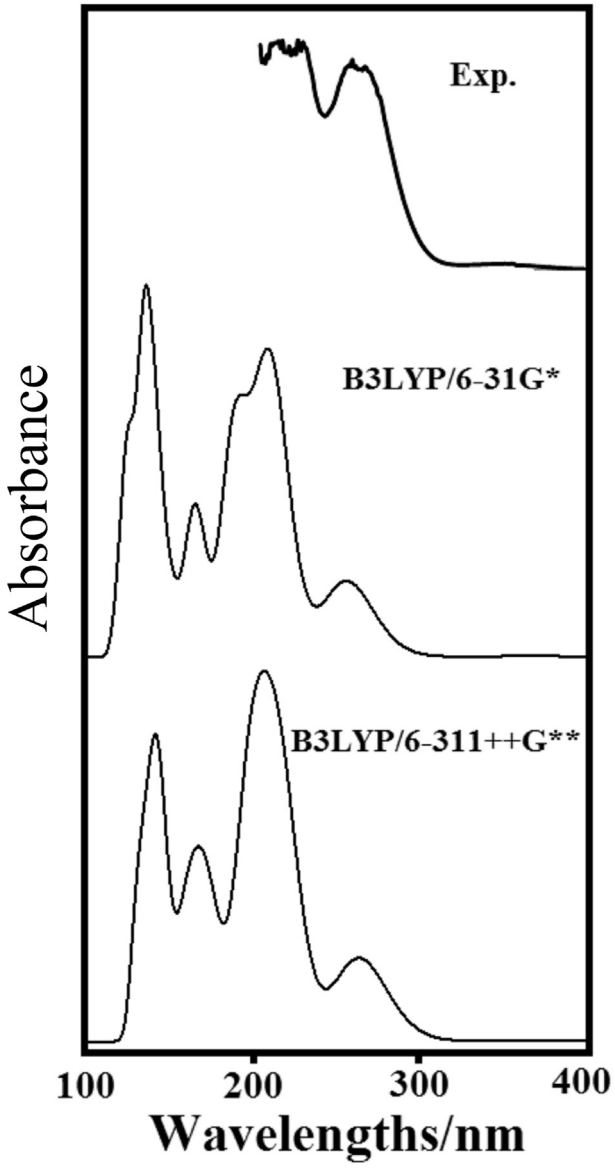

Fig. 5. Experimental UV–visible spectrum of the potassium 3-furoyltrifluoroborate salt in aqueous solution compared with the corresponding predicted in the same media by using B3LYP/6-31G* and B3LYP/6-311++G** levels of theory.

Table S11) increasing the force of the other two bonds and, of course, their corresponding force constants.

6. Electronic spectrum

The predicted UV–visible spectra for FTFB in aqueous solution by using TD-DFT calculations with the B3LYP/6-31G* and B3LYP/6-311++G** methods and the Gaussian program [27] were compared with the corresponding experimental one recorded in the same medium in Fig. 5. The positions of the bands observed in both theoretical and experimental spectra are summarized in Table S10. Experimentally, four bands were observed at 210, 223, 252 and 344 nm where the two first are very intense while the other two have strong and weak intensities. The numbers of the bands predicted by the theoretical calculations are different in gas phase than in aqueous solution and with the different methods. Thus, the spectra in gas phase by using the B3LYP/6-31G* method in aqueous solution predict four bands and two shoulders at 126.3, 136.1, 164.9, 192.7, 208.4 and 255.4 nm where their intensities can be seen in Table S10. Note that with the basis set of higher size the number of bands is reduced to four and those two shoulders could not be seen. The predicted spectra show a reasonable concordance with the experimental ones, especially from the 200–400 nm region because only in that region was recorded the spectra. Evidently, the theoretical spectra are shifted toward lower wavelengths in reference to the experimental one. These bands can be easily assigned to the $\pi \rightarrow \pi^*$ transitions due to the C=C double bonds or to $n \rightarrow \pi^*$ interactions due to the C=O group which are expected in these regions, as suggested by the NBO analysis (Table S3) and, as was assigned in Table S11.

7. Conclusions

In the present work, the potassium 3-furoyltrifluoroborate salt was characterized by means of FT-IR, FT-Raman and UV–Visible spectroscopies. Theoretically the molecular structures in gas phase and in aqueous solution were determined with C_S symmetries by using the B3LYP/6-31G* and B3LYP/6-311++G** methods. Four conformers were found in the potential energy surface but only one of them, named C4, presents the minimum energy and, for this reason, is the most stable. The predicted FT-IR, FT-Raman and UV–visible spectra show very good correlations with the corresponding experimental ones. The predicted solvation energies for the salt by using the B3LYP/6-31G* and B3LYP/6-311++G** methods are −75.79 and −81.55 kJ/mol, respectively. The NBO analyses reveal the high stability of the salt by using the B3LYP/6-31G* level of theory due to $\pi \rightarrow \pi^*$ and $n \rightarrow \pi^*$ interactions attributed to the C=C and C=O double bonds while the AIM studies evidence the ionic characteristics of the salt in both media. The gap values have elucidated that the salt in gas phase is more reactive than in solution, as was reported in the literature while the studies of the charges suggest that the F13···H6 interaction together with the K–O bond could probably modulate the reactivities of this salt in aqueous solution. The force fields were computed with the SQMFF methodology and the Molvib program to perform the complete vibrational analysis. Then, the 39 vibration normal modes classified as 26 A'+ 13 A″ were completely assigned and their force fields and force constants are also reported for the two media by using both levels of theory.

Acknowledgements

This work was supported with grants from CIUNT Project 26/D207 (Consejo de Investigaciones, Universidad Nacional de Tucumán). The authors would like to thank Prof. Tom Sundius for his permission to use MOLVIB.

Appendix A. Supplementary data

Supplementary data related to this article can be found at https://doi.org/10.1016/j.molstruc.2018.01.040.

References

[1] H. Noda, G. Erős, J.W. Bode, Rapid ligations with equimolar reactants in water with the potassium acyltrifluoroborate (KAT) amide formation, J. Am. Chem. Soc. 136 (15) (2014) 5611–5614.
[2] H. Noda, J.W. Bode, Synthesis of chemically and configurationally stable monofluoro acylboronates: effect of ligand structure on their formation, properties, and reactivities, J. Am. Chem. Soc. 137 (11) (2015) 3958–3966.
[3] A.M. Dumas, G.A. Molander, J.W. Bode, Amide-forming ligation of acyltrifluoroborates and hydroxylamines in water, Angew. Chem. 51 (23) (2012) 5683–5686.
[4] I. Pusterla, J.W. Bode, The mechanism of the α-ketoacid-Hydroxylamine amide-forming ligation, Angew. Chem. 51 (2) (2012) 513–516.
[5] A.M. Dumas, G.A. Molander, J.W. Bode, Amide-forming ligation of acyltrifluoroborates and hydroxylamines in water, Angew. Chem. 124 (23) (2012) 5781–5784.
[6] A.M. Dumas, G.A. Molander, J.W. Bode, Amide-forming ligation of acyltrifluoroborates and hydroxylamines in water, Chem. Abstr. 43 (44) (2012).
[7] H. Noda, J.W. Bode, Synthesis and reactivities of monofluoro acylboronates in chemoselective amide bond forming ligation with hydroxylamines, Chem. Abstr. 47 (8) (2016).
[8] D. Romani, I. Salas Tonello, S.A. Brandán, Influence of atomic bonds on the properties of the laxative drug sodium picosulphate, Heliyon 2 (2016) e00190.
[9] A.D. Becke, Density functional thermochemistry. III. The role of exact exchange, J. Chem. Phys. 98 (1993) 5648–5652.
[10] C. Lee, W. Yang, R.G. Parr, Development of the Colle-Salvetti correlation-energy formula into a functional of the electron density, Phys. Rev. B 37 (1988) 785–789.
[11] J. Tomasi, J. Persico, Molecular interactions in solution: an overview of methods based on continous distributions of the solvent, Chem. Rev. 94 (1994) 2027–2094.
[12] S. Miertus, E. Scrocco, J. Tomasi, Electrostatic interaction of a solute with a continuum, Chem. Phys. 55 (1981) 117–129.
[13] A.V. Marenich, C.J. Cramer, D.G. Truhlar, Universal solvation model based on solute electron density and a continuum model of the solvent defined by the bulk dielectric constant and atomic surface tensions, J. Phys. Chem. B113 (2009) 6378–6396.
[14] a) G. Rauhut, P. Pulay, Transferable scaling factors for density functional derived vibrational force fields, J. Phys. Chem. 99 (1995) 3093–3099;
b) G. Rauhut, P. Pulay, J. Phys. Chem. 99 (1995) 14572.
[15] R.G. Parr, R.G. Pearson, Absolute hardness: companion parameter to absolute electronegativity, J. Am. Chem. Soc. 105 (1983) 7512–7516.
[16] J.-L. Brédas, Mind the gap!, Mater. Horiz. 1 (2014) 17–19.
[17] H.A. Höppe, K. Kazmierczak, E. Romano, S.A. Brandán, A structural and vibrational study on the first potassium borosulfate, $K_5[B(SO_4)_4]$ by using the FTIR-Raman and DFT calculations, J. Mol. Struct. 1037 (2013) 294–300. ISSN: 0022-2860.
[18] E. Romano, L. Davies, S.A. Brandán, Structural and vibrational properties of zinc difluoromethanesulfinate. A study combining the FTIR and Raman spectra with ab-initio calculations, J. Mol. Struct. 1044 (2013) 144–151.
[19] E. Romano, F. Ladetto, S.A. Brandán, Structural and Vibrational studies of the potential anticancer agent, 5-difluoromethyl-1,3,4-thiadiazole-2-amino by DFT calculations, Comput. Theoret. Chem. 1011 (2013) 57–64. ISSN: 2210-271/12.
[20] P.G. Cataldo, M.V. Castillo, S.A. Brandán, Quantum mechanical modeling of fluoromethylated-pyrrol derivatives. A study on their reactivities, structures and vibrational properties, J. Phys. Chem. Biophys. 4 (1) (2014) 2–9.
[21] M.J. Márquez, M.B. Márquez, S.A. Brandán, Chapter 6, A structural and spectroscopic study on benzisozaxole methane sulfonic acid sodium salt (BOSNa), in: Silvia A. Brandán (Ed.), Descriptors, Structural and Spectroscopic Properties of Heterocyclic Derivatives of Importance for the Health and the Environmental, Edited Collection, Nova Science Publishers, Inc., 2015, pp. 132–157. ISBN: 978-1-63482-708-9.
[22] A.B. Nielsen, A.J. Holder, GaussView, User's Reference, GAUSSIAN, Inc., Pittsburgh, PA, USA, 2000-2003.
[23] M.J. Frisch, G.W. Trucks, H.B. Schlegel, G.E. Scuseria, M.A. Robb, J.R. Cheeseman, G. Scalmani, V. Barone, B. Mennucci, G.A. Petersson, H. Nakatsuji, M. Caricato, X. Li, H.P. Hratchian, A.F. Izmaylov, J. Bloino, G. Zheng, J.L. Sonnenberg, M. Hada, M. Ehara, K. Toyota, R. Fukuda, J. Hasegawa, M. Ishida, T. Nakajima, Y. Honda, O. Kitao, H. Nakai, T. Vreven, J.A. Montgomery Jr., J.E. Peralta, F. Ogliaro, M. Bearpark, J.J. Heyd, E. Brothers, K.N. Kudin, V.N. Staroverov, R. Kobayashi, J. Normand, K. Raghavachari, A. Rendell, J.C. Burant, S.S. Iyengar, J. Tomasi, M. Cossi, N. Rega, J.M. Millam, M. Klene, J.E. Knox, J.B. Cross, V. Bakken, C. Adamo, J. Jaramillo, R. Gomperts,

R.E. Stratmann, O. Yazyev, A.J. Austin, R. Cammi, C. Pomelli, J.W. Ochterski, R.L. Martin, K. Morokuma, V.G. Zakrzewski, G.A. Voth, P. Salvador, J.J. Dannenberg, S. Dapprich, A.D. Daniels, Ö. Farkas, J.B. Foresman, J.V. Ortiz, J. Cioslowski, D.J. Fox, Gaussian 09, Revision D.01, Gaussian, Inc., Wallingford CT, 2009.

[24] E.D. Gledening, J.K. Badenhoop, A.D. Reed, J.E. Carpenter, F.F. Weinhold, NBO 3.1, Theoretical Chemistry Institute, University of Wisconsin, Madison, WI, 1996.

[25] F. Biegler-Köning, J. Schönbohm, D. Bayles, AIM2000; a program to analyze and visualize atoms in molecules, J. Comput. Chem. 22 (2001) 545.

[26] T. Sundius, Scaling of ab-initio force fields by MOLVIB, Vib. Spectrosc.. 29, 89–95.

[27] D. Romani, S.A. Brandán, Effect of the side chain on the properties from cidofovir to brincidofovir, an experimental antiviral drug against to *Ebola* virus disease, Am. J. Chem. (2015), https://doi.org/10.1016/j.arabjc.2015.06.030.

[28] M.J. Márquez, M.B. Márquez, P.G. Cataldo, S.A. Brandán, A comparative study on the structural and vibrational properties of two cyanopyridine derivatives with potentials antimicrobial and anticancer activities, OJSTA 4 (2015) 1–19.

[29] D. Romani, S.A. Brandán, M.J. Márquez, M.B. Márquez, Structural, topological and vibrational properties of an isothiazole derivatives series with antiviral activities, J. Mol. Struct. 1100 (2015) 279–289.

[30] D. Romani, S.A. Brandán, Structural, electronic and vibrational studies of two 1,3-benzothiazole tautomers with potential antimicrobial activity in aqueous and organic solvents. Prediction of their reactivities, Comput. Theor. Chem. 1061 (2015) 89–99.

[31] P. Ugliengo, MOLDRAW Program, University of Torino, Dipartimento Chimica IFM, Torino, Italy, 1998.

[32] 4-methylbenzoylboronate (E)-1-(((4-bromophenyl)imino)methyl)naphthalen-2-o.

[33] 4-methylbenzoylboronate (E)-2-(((2-(Hydroxymethyl)phenyl)imino)methyl) phenol.

[34] H. Ghalla, N. Issaoui, M.V. Castillo, S.A. Brandán, H.T. Flakus, A complete assignment of the vibrational spectra of 2-furoic acid based on the structures of the more stable monomer and dimmer, Spectrochim. Acta Part A 121 (2014) 623–631.

[35] R.F.W. Bader, Atoms in Molecules. A Quantum Theory, Oxford University Press, Oxford, 1990. ISBN: 0198558651.

[36] G. Keresztury, S. Holly, G. Besenyei, J. Varga, A.Y. Wang, J.R. Durig, Vibrational spectra of monothiocarbamates-II. IR and Raman spectra, vibrational assignment, conformational analysis and *ab initio* calculations of *S*-methyl-*N*,*N*-dimethylthiocarbamate, Spectrochim. Acta 49A (1993) 2007–2026.

[37] D. Michalska, R. Wysokinski, The prediction of Raman spectra of platinum(II) anticancer drugs by density functional theory, Chem. Phys. Lett. 403 (2005).